Effects of the architecture of tissue engineering scaffolds on cell seeding and culturing

Ferry P.W. Melchels[1#], Ana M.C. Barradas[2], Clemens A. van Blitterswijk[2], Jan de Boer[2], Jan Feijen[1] and Dirk W. Grijpma*[1,3]

1. MIRA Institute for Biomedical Technology and Technical Medicine, Department of Polymer Chemistry and Biomaterials, University of Twente, P.O. Box 217, 7500 AE, Enschede, The Netherlands

j.feijen@utwente.nl; d.w.grijpma@tnw.utwente.nl

2. MIRA Institute for Biomedical Technology and Technical Medicine, Department of Tissue Regeneration, University of Twente, P.O. Box 217, 7500 AE, Enschede, The Netherlands

a.m.c.barradas@tnw.utwente.nl; c.a.vanblitterswijk@tnw.utwente.nl; j.deboer@tnw.utwente.nl

3. Department of Biomedical Engineering, University Medical Centre Groningen and University of Groningen, P.O. Box 196, 9700 AD Groningen, The Netherlands

* Corresponding author: Prof. Dr. Dirk W. Grijpma, tel. +31 53 489 2966, fax. +31 53 489 2155

current address: Institute of Health and Biomedical Innovation, Department of Regenerative Medicine, Queensland University of Technology, 60 Musk Avenue, Kelvin Grove, QLD 4059 Australia.

ferry.melchels@qut.edu.au

Abstract

The advance of rapid prototyping techniques has significantly improved control over the pore network architecture of tissue engineering scaffolds. In this work we assessed the influence of scaffold pore architecture on cell seeding and static culturing, by comparing a computer-designed gyroid architecture fabricated by stereolithography to a random-pore architecture resulting from salt-leaching. The scaffold types showed comparable porosity and pore size values, but the gyroid type showed a more than tenfold higher permeability due to the absence of size-limiting pore interconnections. The higher permeability significantly improved the wetting properties of the hydrophobic scaffolds, and increased the settling speed of cells upon static seeding of immortalised mesenchymal stem cells. After dynamic seeding followed by 5 days of static culture, gyroid scaffolds showed large cell populations in the centre of the scaffold, while salt-leached scaffolds were covered with a cell-sheet on the outside and no cells were found in the scaffold centre. It was shown that interconnectivity of the pores and permeability of the scaffold prolongs the time of static culture before overgrowth of cells at the scaffold periphery occurs. Furthermore, novel scaffold designs are proposed to further improve the transport of oxygen and nutrients throughout the scaffolds, and to create tissue engineering grafts with designed, pre-fabricated vasculature.

Keywords: scaffold architecture, computer-aided design, cell seeding, hypoxia, nutrient transport

Introduction

In tissue engineering, two major challenges are the homogeneous seeding of cells throughout a porous scaffold, and to provide the seeded cells with sufficient oxygen and nutrients to sustain, proliferate and generate new tissue. Several methods have been proposed for the seeding of cells into microporous scaffolds. Static seeding –although still widely used- is characterised by low cell seeding efficiencies and inhomogeneous distributions [1, 2]. An improvement in both seeded cell density and uniformity of the distribution can be achieved by employing mild suction to inoculate cells into a porous scaffold [3]. A similar technique that showed good results but is only possible when using elastomeric scaffolds, is compression-induced suction [4]. Furthermore, several dynamic seeding methods have been developed using for example spinner flasks [2, 5] or perfusion bioreactors [6]. Besides the technique employed for cell seeding, the scaffold architecture and physical properties of the scaffolding material play an important role in the cell seeding procedure [7]. Most polymers used for tissue engineering scaffolds (such as poly(lactide), poly(ε-caprolactone) and poly(trimethylene carbonate)) are hydrophobic, which impedes the penetration of an aqueous cell suspension. These materials are often incubated in culture medium prior to cell seeding, in order to let proteins adsorb that make the scaffold surface less hydrophobic and improve cell attachment [8]. An open, permeable pore network architecture facilitates wetting by culture medium and aids in eventually achieving high densities of uniformly distributed cells upon seeding. Moreover, it can improve oxygen and nutrient transport in the culturing phase [9]. In static culture of cell-seeded porous scaffolds, cells that are too far from the periphery often go into necrosis because of hypoxia or lack of nutrients. Due to the diffusion constraints of foams fabricated using conventional techniques such as salt-leaching and phase-separation/freeze-drying, only the in vitro growth of tissues with cross-sections of less than 500 µm have proven successful in static culture [10, 11]. Cell colonisation at the scaffold periphery can consume, or act as an effective barrier for the diffusion of oxygen and nutrients into the interior of the scaffold [12]. Perfusion of medium through scaffolds in

a bioreactor has been suggested to overcome cell death due to transport limitations [13]. It can increase the survival rate of cells in the centre of porous scaffolds, resulting in more homogeneous tissue engineered constructs [14]. However, perfusion alone is not always enough to ensure adequate oxygen supply inside porous scaffolds [15]. The use of solid freeform fabrication (SFF) or rapid prototyping (RP) techniques such as stereolithography may be an attractive approach to produce scaffolds with customised external shape and predefined and reproducible internal morphology. The pore networks of such scaffolds may be designed such to reduce resistance to mass transport by shortening diffusion paths (lower tortuosity) and increasing pore interconnectivity size [16]. In stereolithography, a computer-controlled laser beam or a digital light projector is used to locally solidify a liquid resin through photo-initiated polymerisation. In combination with a computer-driven building stage, a solid, three-dimensional object can be constructed in a layer-by-layer fashion [17]. Recently, we have reported the use of stereolithography and methacrylate end-functionalised poly(D,L-lactide) (PDLLA) oligomers to fabricate tissue engineering scaffolds by computer-aided designs (CAD) [18].

We aim to improve the scaffold architecture such that cell-seeded scaffolds can be cultured for prolonged time under static conditions, providing the proliferating cells with sufficient oxygen and nutrients. We use stereolithography to prepare highly accessible and permeable porous scaffolds of poly(D,L-lactide) and compare their cell seeding and cell culturing characteristics with more tortuous scaffolds prepared using the salt-leaching technique. The latter method is widely used to prepare porous tissue engineering scaffolds but has limited control of the pore network architecture [19]. Cell survival and proliferation are expected to improve for the more accessible architectures.

Materials and Methods

Scaffolds

A liquid photo-polymerisable resin based on poly (D,L-lactide) (PDLLA) was synthesised in a similar way as previously described [18]. In short, 1,6-hexanediol (Sigma-Aldrich) and D,L-lactide (Purac) were reacted at 130 °C for 40 h under an argon atmosphere using stannous octoate (Sigma-Aldrich) as a catalyst. The hydroxyl termini of the oligomers were reacted with methacrylic anhydride (Sigma-Aldrich) in the presence of triethyl amine (Sigma-Aldrich) (both in a 20 mol % excess) in dried dichloromethane for 5 d at room temperature to yield methacrylate end-functionalised lactide macromers. These were purified by precipitation from isopropanol followed by washing with water and freeze-drying. ^{1}H-NMR ($CDCl_3$, Varian 300 MHz) indicated high purity, a molecular weight of 5 kg/mol and a degree of functionalisation of 92-99 %. The macromers were used to prepare a photo-polymerisable liquid resin with 40 wt% dry N-methylpyrrolidone (NMP, Fluka) as a non-reactive diluent, 2 wt% ethyl-2,4,6-trimethylbenzoylphenylphosphinate (Lucirin TPO-L photo-initiator, gift from BASF), 0.15 wt% Orasol Orange G dye (gift from Ciba SC) to control the cure depth and 0.2 wt% tocopherol (Fluka) to prevent preliminary crosslinking reactions.

A scaffold design with an open and accessible gyroid architecture was generated using K3dSurf v0.6.2 software (http://k3dsurf.sourceforge.net). The surface of the gyroid pore architecture is described by a triply periodic function, closely approximating the minimal surfaces of Schwarz and Schoen [20, 21]. Addition of an offset value to the implicit function allows designing porous structures having specific porosities. A value of -0.60 was chosen for the offset, corresponding to 70 % porosity. The following equation was used to describe the scaffold design:

$$G : \cos(x)\sin(y) + \cos(y)\sin(z) + \cos(z)\sin(x) - 0.60 = 0$$

with boundary conditions $x^2 + y^2 < (14\pi)^2$ and $|z| < 10\pi$. A commercial stereolithography apparatus (Envisiontec Perfactory Mini Multilens SLA) was employed to build the designed gyroid scaffolds using the PDLLA-based resin. The building process involves subsequent projections of 1280x1024 pixels, each 32x32 μm^2 in size. Layers with a thickness of 25 μm were cured by irradiating for 30 s with blue light (intensity 16 mW/cm^2). Uncured excess resin was washed out and the diluent, non-reacted macromer and photo-initiator were extracted from the structures with acetone. The extracted structures with a height of 5 mm and a diameter of 8 mm were then dried at 90 °C for 2 d under a nitrogen flow. A similar resin, without dye and containing camphorquinone (also 2 wt%) instead of Lucirin TPO-L, was used to prepare porous structures by a salt-leaching process. The resin was mixed with NaCl salt particles sieved to sizes of 425-710 μm, in a 1:3.5 weight ratio. The size range and weight ratio was chosen such that a porosity and average pore size similar to that of the stereolithography-built scaffolds was obtained. Then the mixture was brought into tubular polypropylene moulds (inner diameter 14 mm) and cured by irradiation through the tube wall with a Kerr dental light (mono-chromatic blue LED light, wavelength 470 nm, intensity 1000 mW/cm2) for 40 s. The specimens were frozen in liquid nitrogen, cut to the desired dimensions, and post-cured by heating to 90 °C for 12 h. The salt-containing composites were extracted in acetone for 2 d, and the salt fraction was leached out with water during a period of 7 d. Then, the porous structures with the same final approximate dimensions as the built gyroid scaffolds were dried at 90 °C for 2 d under a nitrogen flow.

Structural analyses were performed on the fabricated scaffolds by micro computed tomography (μCT) using a General Electric eXplore Locus SP scanner at 14.3 μm resolution. The scan was carried out at a voltage of 80 kV, a current of 80 μA and an exposure time of 3000 ms. No filter was applied. The scanned data was reconstructed with a Feldkamp-based algorithm to obtain three-dimensional images and for the calculation of porosities, pore size distributions and pore accessibility.

The resistance to water flow was determined for both scaffold types by measuring the time required for a fixed volume of water to flow through a fully pre-wetted scaffold inserted in a silicone rubber tube. Permeabilities were calculated using Darcy's law:

$$Q = -\kappa \frac{\Delta P}{\mu} \frac{A}{L}$$

where κ is the scaffold permeability (mm^2), Q is the flow rate (mm^3/s), μ the viscosity of water (0.001 Ns/mm^2 at room temperature), ΔP the pressure difference (N/mm^2), A the cross-section surface area (mm^2) and L the scaffold height (mm).

iMSC culturing

Telomerase immortalised bone marrow derived mesenchymal stromal cells (iMSC) were kindly provided by Prof. Dr. Ola Myklebost (University of Oslo, Norway). Cells were expanded and cultured in proliferation medium consisting of α-MEM (Gibco), 10 % foetal bovine serum (FBS, Lonza), 2 mM L-glutamine (Gibco), 0.2 mM ascorbic acid (Sigma, A8960), 100 u/mL penicillin and 100 g/mL streptomycin (Gibco) and 1 ng/mL bFGF (Instruchemie). Medium was refreshed 3 times per week and cells were trypsinised whenever a confluency of 70-80% was reached. Standard culturing conditions were 37 ºC and a 5 % CO_2, 100% humid atmosphere.

Scaffold cell seeding

In previous work, the photo-crosslinked polylactide network material was shown to be a non-cytotoxic substrate that allows for good cell spreading and proliferation [18]. The scaffolds were disinfected in 70% isopropanol for 15 min. However, salt-leached scaffolds were not wetted throughout the porous structures by this procedure and were therefore wetted and simultaneously disinfected using ethanol and vacuum-release cycles (see Results and Discussion section). The disinfected scaffolds were washed two times one hour in large quantities of PBS on an orbital

shaker, and incubated in proliferation medium overnight to allow protein adsorption on its surface. For both seeding methods, iMSC were trypsinised and resuspended in proliferation medium at a concentration of 4×10^5 cells per scaffold seeding volume. Scaffolds were seeded both statically and dynamically (**Fig. 1**). For static seeding, the seeding volume per scaffold was 60 µl, corresponding to 40 % of the pore volume of a scaffold (obtained from µCT data). The cell suspension was pipetted on top of the scaffolds that were placed each in a well of 4 cm^2 non cell-adherent polystyrene surface, and left to incubate for 4 h under standard culturing conditions. For the dynamic seeding, the seeding volume was 150 µl, corresponding to the full scaffold pore volume (obtained from µCT data). A scaffold was placed in a 2 mL syringe (Ø 8.7 mm) and one seeding volume of cell suspension was pipetted on top of the scaffold. Then a second scaffold was inserted on top of the first, followed again by one seeding volume of cell suspension. These steps were repeated up to 5 stacked scaffolds + 5 seeding volumes per syringe. After putting the scaffolds and cell suspension seeding volumes in the syringe tube, the plunger was pushed inside to expel the air bubbles trapped in the tube, and the tube tip was closed with a cap. The syringes were placed horizontally on a roller (0.5 Hz) under standard culturing conditions for 4 h to allow cell attachment onto the scaffolds.

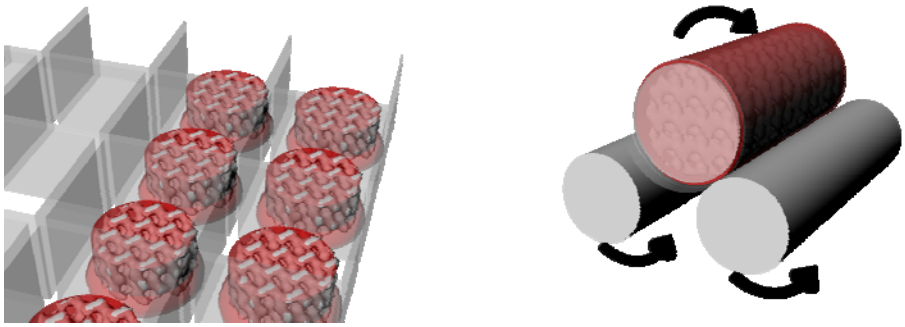

Fig. 1. **Schematic diagram of static seeding (left) and dynamic seeding (right). In the static seeding procedure, cell suspensions were pipetted on top of the scaffolds and left to stand for 4 h in an incubator. In the dynamic seeding procedure, the cell suspensions were pipetted on the scaffolds while sitting inside a syringe tube, followed by incubation on a roller (0.5Hz) for 4 h.**

Static culturing

iMSC were seeded dynamically and after a 4 h incubation period, the scaffolds were taken out from the syringes and placed individually in empty wells of 4 cm^2 surface. Non-treated polystyrene well plates with ultra low cell adherence were employed to prevent growth of cells in the wells, competing for nutrients and oxygen. Two mL of proliferation medium was added per well to all scaffolds, followed by standard culturing conditions for 20 d. Medium was refreshed 3 times per week, and 5 scaffolds of each type were taken out after 5, 10 and 20 d.

DNA Assay

Medium was aspirated from the wells and the scaffolds were washed once in PBS from 3 samples per time point in the culturing experiment. After incubation at -80 ºC overnight to ensure cell lysis, 600 µL of 1× cell lysis buffer (CyQUANT®, Invitrogen) containing 1.35 Ribonuclease A Kunitz units/mL (Sigma Aldrich) was added to the scaffolds and incubated for 1 h on a shaking platform to assure that all cell content was released from the scaffold to the buffer solution. Next, 100 µL of 8×CyQUANT® dye was added to 100 µL of cell lysate and incubated for 15 min at room temperature in the dark. Fluorescence measurements were performed at 480/520 nm of excitation/emission peaks respectively.

Methylene blue staining, sectioning and imaging

Medium was aspirated from the wells and the scaffolds were washed once in PBS. Afterwards, scaffolds were incubated in HistoChoice fixative solution (Sigma Aldrich) for 20 min followed by washing in PBS. The scaffolds were immersed in a 1% methylene blue solution for 1 min after which they were washed several times in PBS until no blue staining came out of the scaffold. The stained scaffolds were visualised using a stereomicroscope (Nikon SMZ-10A with Sony 3CCD camera), both before and after sectioning through the middle using a diamond saw (Leica SP1600).

Hypoxia assay with A4-4 cells

A biological reporter system was used to compare hypoxic conditions in scaffolds with different architectures. The Hypoxia Responsive Element-Luciferase (HRE-Luc) transfected Chinese Hamster Ovary (CHO) A4-4 cell line [22] was kindly provided by Dr. Kiyoshi Nose (Showa University, Tokyo, Japan). The (HRE) promoter depends on hypoxia-inducible factor 1 (HIF1), of which the activity is regulated by the partial O_2 pressure in the cell. By adding luciferin to the cell lysate, light emission occurs as result of the luciferase-luciferin reaction. The intensity is a measure for the amount of luciferase expressed and for the lack of O_2 available for the cells.

A4-4 cells were cultured in α-minimum essential medium (Gibco) supplemented with 10% FBS (Lonza), 2 mM L-glutamine (Life Technologies), 100 U/mL penicillin (Life Technologies) and 10 μg/mL streptomycin (Life Technologies). The medium was refreshed 3 times per week, and the cells were grown under standard culturing conditions. For seeding of the scaffolds, the cells were trypsinised and $3.0 \cdot 10^5$ cells in 60 μL of medium were pipetted on top of each scaffold, which was placed in wells of non cell-adherent polystyrene plates and left to attach for 4 hours before adding additional culture medium. After 5 days, the cells were lysed and the luciferase activity was analysed according to the protocol of the luciferase assay kit (Promega). Luminescence was measured using a Bio-orbit 1253 Luminometer (ABOATOX). The luciferase activity was calculated in triplicate, normalising the luciferase activity to the DNA amounts from the same cell lysate, following the DNA assay procedure described above.

Results and Discussion

Scaffold architecture characterisation

The synthesised PDLLA-dimethacrylate macromer was used to prepare liquid resins for the stereolithography fabrication and for the preparation of porous scaffolds by photo-polymerisation and salt-leaching. After preparing both scaffold types, micro computed tomography (μCT) was used to obtain visualisations and quantitative data to characterise the pore networks of the scaffolds (**Fig. 2**).

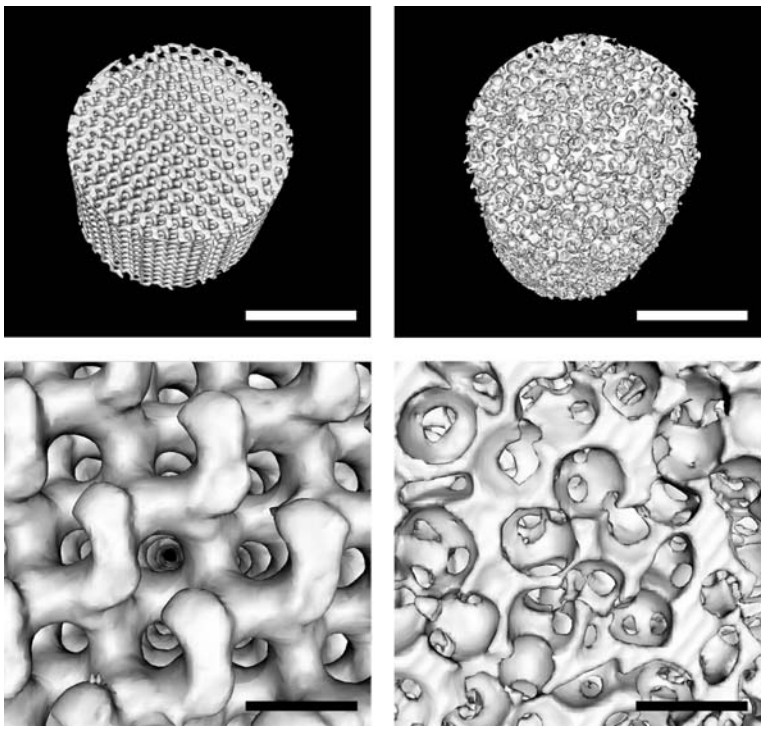

Fig. 2. **μCT-visualisations of gyroid scaffolds prepared by stereolithography (left) and salt-leached scaffolds (right), showing pores and pore interconnections. Scale bars are 4 mm (top) and 500 μm (bottom).**

Table 1 shows parameters related to the pore network architecture of both scaffold types. The processing parameters for the preparation of both scaffold types were chosen such that a similar porosity and average pore size were obtained, in order to assess solely the effect of pore network

architecture on cell seeding and culturing characteristics. Nevertheless, the salt-leached scaffolds have a higher specific surface area, as a result of the more random architecture of pores and pore walls as opposed to the designed gyroid architecture. A relative low surface area is one of the major restrictions of uniform tissue engineering scaffolds prepared by rapid prototyping techniques. For example, some researchers have combined a fibre plotting technique with elecotrospun fibres to increase the surface area available for cell attachment [23]. The stereolithography technique used here has a higher resolution than most other rapid prototyping techniques, resulting in a specific surface area that is not more than 28 % lower than that of salt-leached structures at similar porosity and pore size. Furthermore, not all surface area in porous structures is available to cells, as cells usually do not enter pores with interconnections that are less than 5 to 10 times the diameter of a cell. After applying a threshold of 100 μm for pore interconnection size, the specific surface area remaining available to cells is even slightly higher for the gyroid type scaffold than for the salt-leached type scaffold.

Table 1: Structural parameters for both scaffold architectures, obtained from micro-computed tomography scanning data. Values are average ± standard deviation of 5 samples.

	porosity (vol%)	specific surface area (mm^{-1})		average pore size (μm)
		45 μm threshold	100 μm threshold	
gyroid	67.5 ± 3.8	10.0 ± 1.3	9.1 ± 1.2	255 ± 25
salt-leached	68.9 ± 4.4	14.0 ± 1.4	8.5 ± 1.6	290 ± 11

Fig. 3 shows pore size distributions of the gyroid and salt-leached scaffolds as a histogram. The salt-leached scaffold shows a typical pore size distribution of scaffolds prepared by porogen leaching methods. Salt particles are sieved and one fraction (in this case 425-725 μm) is mixed with the polymer solution to make a composite. Leaching of the salt and extraction of the diluent then results

in pores having a range of pore sizes. The gyroid architecture contains channels having approximately the same diameter throughout the structure, resulting in a smaller pore size distribution. This is also expressed by the standard deviation, that is 76±3 μm for the gyroid scaffold and 126±8 μm for the salt-leached scaffold (both n=5).

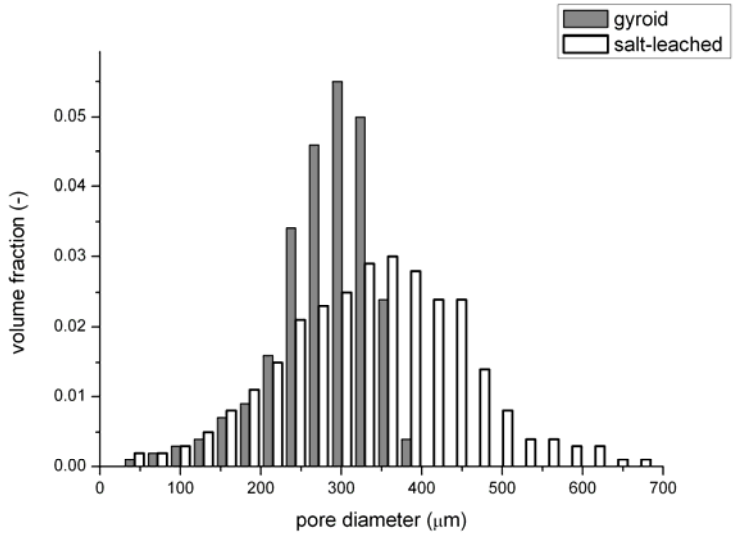

Fig. 3. **Pore size distributions of the gyroid and salt-leached scaffolds, obtained from μCT scanning data (average of 5 samples).**

Despite the slightly smaller pore sizes in the prepared gyroid scaffolds, this scaffold architecture has a more open and accessible pore network. The number, size and location of the interconnections between pores play an important role in cell seeding, and in nutrient transport and cell migration during the cell culturing phase. While the gyroid pore network consists of channels with no clear boundaries between pores, the pore network of salt-leached scaffolds has interconnections smaller than the pores themselves, as can be clearly seen in **Fig. 2**. These small pore interconnections impede flow; therefore the two scaffold architectures show a large difference in permeability, despite of the similar porosity and pore size. For both scaffold types, the resistance to water flow through the scaffold was measured. The resulting permeabilities are 0.519 ± 0.045 mm^2 for the

gyroid scaffold and 0.046 ± 0.007 mm^2 for the salt-leached scaffold (both n=5). The large difference of more than 1 order of magnitude indicates the strong influence of scaffold architecture on transport phenomena.

Effect of wetting properties on cell seeding behaviour

iMSC were statically seeded by pipetting a cell suspension on top of both salt-leached scaffolds and gyroid scaffolds prepared by stereolithography. Prior to seeding, the scaffolds were disinfected in 70 % isopropanol, washed twice with PBS and incubated in culture medium overnight. The tortuous salt-leached scaffolds floated in all these liquids, indicating trapped air inside the scaffold as a result of poor wetting. As a consequence, the cell suspension did not penetrate deep into the scaffolds and cells were only found on the outside surface. The open gyroid scaffolds, however, were easily wetted by the isopropanol/water mixture, as well as by PBS and by culture medium, although PDLLA is a hydrophobic material. This allowed for intrusion of the cell suspension deep into the scaffolds, and cells were distributed all throughout. This is clearly seen in **Fig. 4**, where blue stained areas indicate the presence of adhered cells.

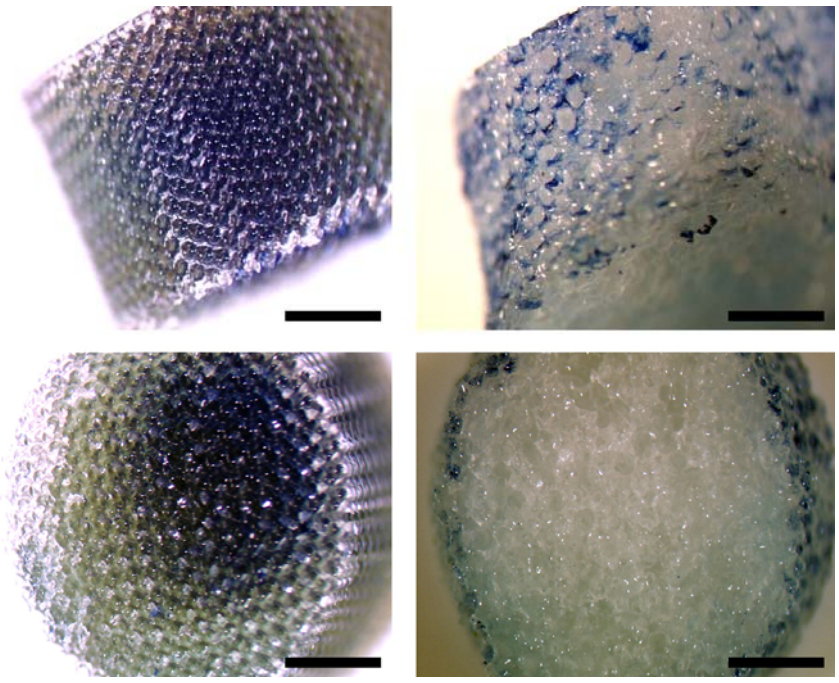

Fig. 4. **Stereomicroscope images of methylene blue-stained cells on gyroid (left) and salt-leached (right) scaffolds after static seeding. Top row: images were taken from the outside (side-views). Bottom row: images were taken from the middle cross-section of the scaffold. Scale bars are 2 mm.**

The results demonstrate that the open architecture of the gyroid scaffold facilitates the infiltration of a cell suspension into the scaffold, despite its hydrophobic nature (poly(D,L-lactide has a contact angle of 74 ° [24]). Highly tortuous porous structures -such as salt-leached scaffolds- prepared from hydrophobic materials need extensive pre-treatment to ensure good wetting before cells can be seeded deeper into the scaffold [25]. All further seeding experiments on salt-leached scaffolds were performed after such pre-wetting treatment, as described below.

Static vs. dynamic seeding of iMSC on scaffolds

Cell seeding of both scaffold types was compared under static and dynamic conditions, after performing pre-wetting on the salt-leached scaffolds. Several evacuation-pressure release cycles were performed on the scaffolds in ethanol, to remove all air from the pores. Ethanol was then gradually replaced by PBS, leaving the scaffolds agitated for several hours to ensure adequate liquid exchange between the pores and the bulk liquid outside the scaffold. Finally, PBS was replaced by culture medium and incubated overnight, prior to cell-seeding. For the static seeding, a cell suspension was pipetted on top of the scaffold and left to attach for 4 h. For the dynamic seeding, cell suspensions were pipetted on top of scaffolds inserted in syringe tubes that were incubated on a roller (0.5 Hz) for 4 h. Images obtained by stereomicroscopy show methylene blue staining after both static (**Fig. 5**) and dynamic (**Fig. 6**) seeding.

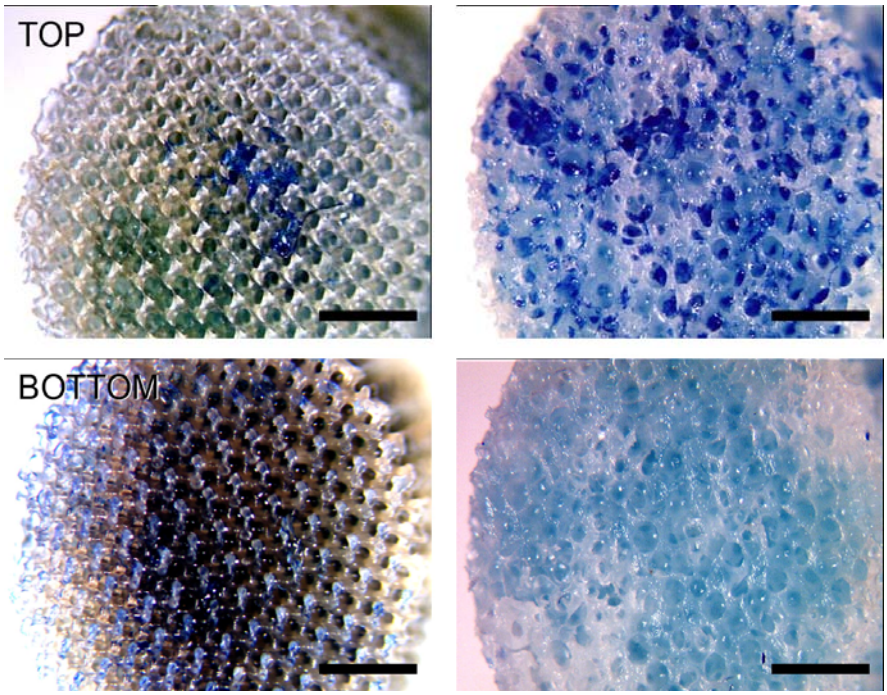

Fig 5. **Stereomicroscope images of methylene blue-stained cells on gyroid (left) and salt-leached (right) scaffolds after static seeding. Images were taken from the top and bottom of the scaffold. Scale bars are 2 mm.**

In the static seeding results, there is a clear effect of scaffold permeability on final cell distribution. For the very open gyroid scaffold, large cell clusters were found on the bottom of the scaffold, and below the scaffold in the well. The very open architecture does not allow sufficiently long entrapment of the cells, so many cells sink to the bottom before they are able to attach to the surface-adsorbed proteins. For the salt-leached scaffolds, the opposite is true. The cells sink into the scaffold, but due to the tortuous architecture they are retained in the upper part. Consequently, cell adhesion occurs here and confines the distribution of cells to this region. The permeability for which this static seeding procedure results in an optimal cell distribution lies in between those of the investigated scaffold types. However, the seeding kinetics cannot be altered without changing also the accessibility of the scaffold for nutrients etc., so other seeding methods are desired.

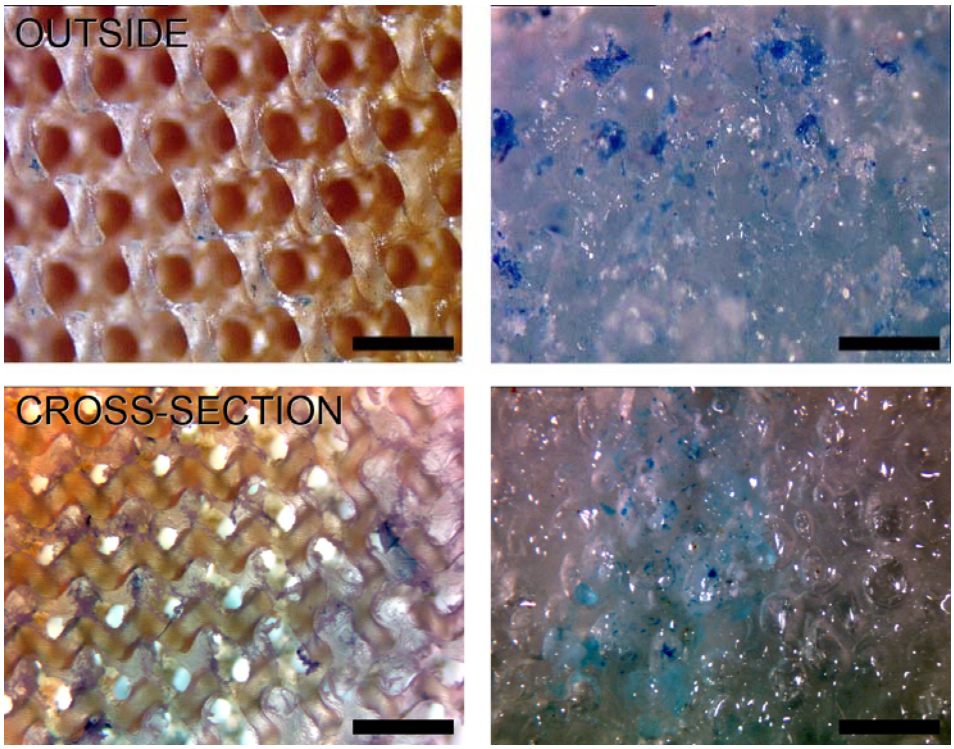

Fig. 6. **Stereomicroscope images of methylene blue-stained cells on gyroid (left) and salt-leached (right) scaffolds after dynamic seeding. Top row: images were taken from the outside of the scaffold. Bottom row: images were taken from the middle cross-section of the scaffold. Scale bars are 500 μm.**

Using the dynamic method, the gyroid scaffold is seeded very homogeneously, much more than with the static method. The absence of intense blue coloured areas indicates the absence of clusters with high cell densities (**Fig. 6**). In the salt-leached scaffold, cells are also distributed more homogeneously than by static seeding, although the cells are still found in clusters. Overall, we observe that dynamic seeding increases the homogeneity of the seeding, and a regular open architecture adds to a homogeneous seeding of cells.

Static culturing of iMSC on scaffolds

Since transport limitations are mostly pronounced under static conditions and these are the prevailing method in the tissue engineering practice, we chose to assess the influence of scaffold

architecture in static culturing. Gyroid scaffolds and salt-leached scaffolds were seeded dynamically for 4 h in syringes on a roller. Then the cells were cultured statically in non-adherent tissue culture plates and medium was refreshed 3 times per week. Samples were taken for methylene blue staining after seeding (4 h) and after 5, 10 and 20 d of culture. In **Fig. 7**, microscopy images depict methylene blue-staining after 5 d of culture, both on the outside as well as on cross-sections of the middle of the scaffolds. After a 5 d culture period, a large increase in cell density can be seen on the outside for both scaffold types, as compared to the scaffolds just after seeding (**Fig. 6**). However, the middle cross-sections show a clear difference between both scaffold architectures. In the gyroid scaffold, many cells can be seen distributed throughout the central part of the scaffold. In the middle section of the salt-leached scaffold however, hardly any cells can be observed. The outer pores of the salt-leached scaffolds are filled with cells and deposited matrix, thereby blocking the inside of the scaffold from inflow of oxygenated and nutrient-rich medium [12]. The small interconnections to deeper pores are completely obstructed. In the gyroid scaffold the pore channels are still open, allowing the supply of nutrients and oxygen to the cells inside the scaffold. The much higher cell number for the gyroid scaffolds was confirmed by a DNA assay, where an absorbance of 34 ± 7 a.u. was measured for the gyroid scaffolds as opposed to 16 ± 1 a.u. for the salt-leached scaffolds at day 5.

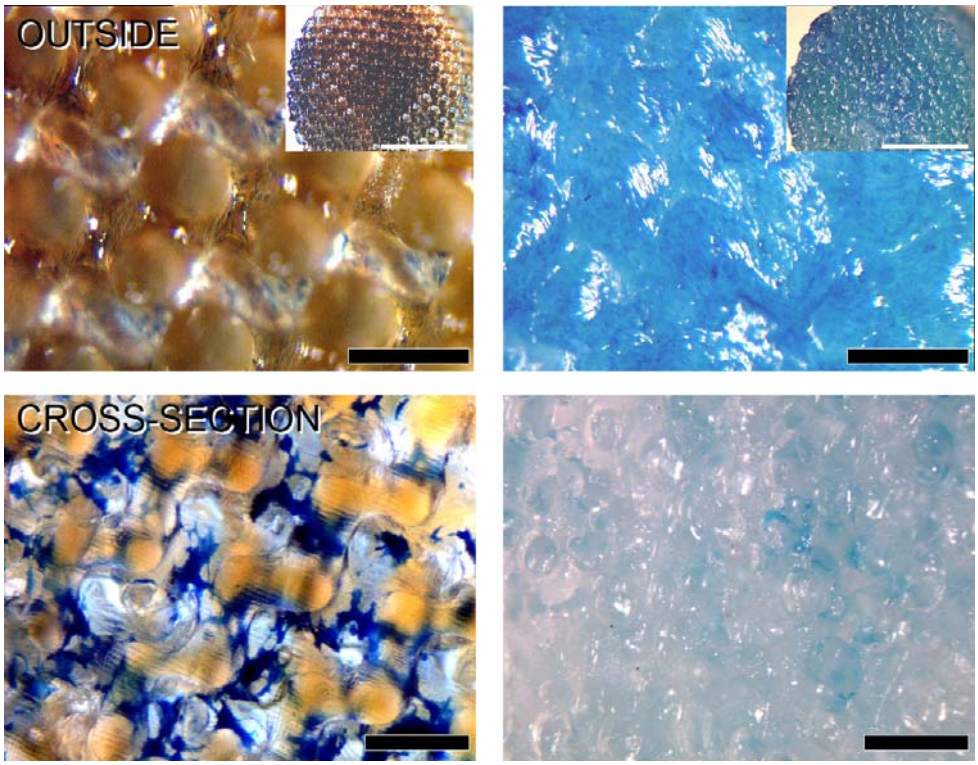

Fig. 7. **Stereomicroscope images of methylene blue-stained cells on gyroid (left) and salt-leached (right) scaffolds after 5 days of static culture. Top row: images were taken from the outside of the scaffold. Bottom row: images were taken from the middle cross-section of the scaffold. Scale bars are 500 μm or 4 mm in the inserts above.**

Here, the benefit of open scaffold architectures on static cell culturing is clearly shown. Whereas the salt-leached scaffolds were totally blocked with cells and deposited matrix within 5 d, the channels in the gyroid scaffold were still accessible. This allowed for sufficient supply of oxygen and nutrients for cells in the centre of the scaffold to proliferate significantly (**Fig. 7)**.

Above, the benefit of well-defined, permeable scaffold pore architectures is shown, as it increases the period that cells inside a scaffold can access sufficient nutrients and oxygen, as compared to random-pore architectures with similar pore sizes. The possibility to culture cell-seeded scaffolds for at least 5 days provides an advantage for tissue engineering purposes. In bone tissue engineering, for instance, the *in vivo* bone forming potential of cells is often assessed by seeding them on

scaffolds, followed by *in vitro* culturing for 7 days prior to implantation in an animal model [26]. Researchers frequently use scaffolds with poorly defined architectures, which compromises the quality of the tissue engineered grafts and the success of the *in vivo* bone formation. Here we present a designed gyroid scaffold that very well suits this application, as it guarantees good cell distribution and proliferation in a period of time that is common practice in tissue engineering applications.

After showing that the larger pore interconnections of the gyroid scaffolds as compared to those of the salt-leached scaffolds are advantageous regarding cell distribution and proliferation, we further assessed how larger pore interconnections and improved permeability of gyroid scaffolds could influence oxygen levels throughout the scaffold. For this, we used A4-4 cells that express luciferase in an O_2 concentration-dependent manner. The amount of expressed enzyme can be measured by quantifying the emitted light, resultant from the luciferase-luciferin reaction that depends on the availability of O_2 in the extracellular milieu. Gyroid scaffolds of two different average pore sizes were used to seed and culture A4-4 cells. After 5 days, the cells on the scaffolds with smaller pores (270 μm) expressed considerably more luciferase per cell than those with larger pores (350 μm), indicating different levels of available oxygen for the cells. This data clearly shows how a rationally designed architecture can substantially improve the culturing conditions of cells.

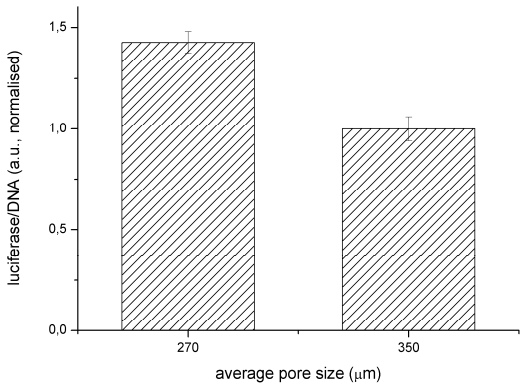

Fig. 8. **Luciferase activity of A4-4 cells cultured for 5 days on PDLLA gyroid scaffolds for two different average pore sizes. The data are based on 3 scaffolds each and normalised to amount of DNA.**

Outlook

Although 5 days cultures showed encouraging results, after prolonged static culture of 20 days also gyroid scaffolds were found covered with a dense film of cells and matrix, with no surviving cells inside the scaffold (**Fig. 9**). This suggests that for prolonged culturing periods, static culturing of any scaffold with sizes of several mm will not lead to mature tissue with living cells throughout, regardless of pore architecture. However, the combination of a rationally designed scaffold architecture and active perfusion could improve cell viability throughout such constructs *in vitro* and, moreover, could facilitate invasion of the graft by the vasculature of the host. The penetration of natural capillary blood vessel networks with oxygen and nutrients enriched blood connected to the main vasculature will ultimately ensure cell survival upon implantation.

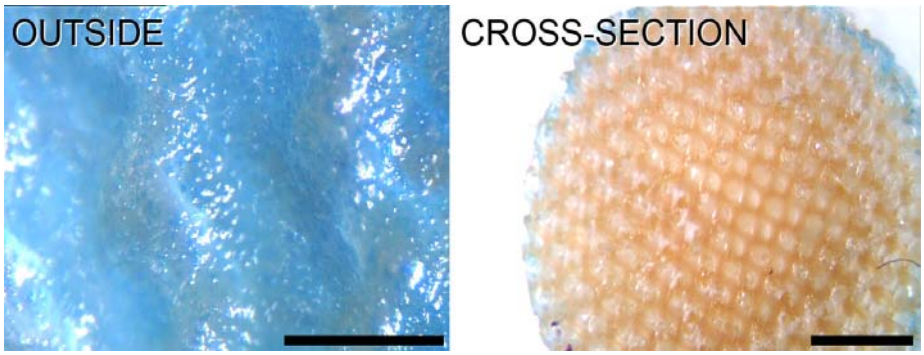

Fig. 9. **Stereomicroscope images of methylene blue-stained cells on gyroid scaffolds after 20 d of static culture. Scale bars are 500 μm (left) and 2 mm (right).**

No cells, except for chondrocytes, exist further than 25-100 μm away from a blood supply [27] in order to access nutrients and oxygen. Therefore, we believe that tissue engineering scaffolds should embrace nature´s approach and mimic the vascular system present to increase the mass transport of oxygen and nutrients deep within and removal of waste products from the scaffold. To achieve such scaffold design, freeform fabrication can play a role [16]. In **Fig. 10** we present a novel scaffold design where we combine meso-scale pores (250 μm) in which cells can proliferate and deposit matrix, with macro-scale channels (600 μm).

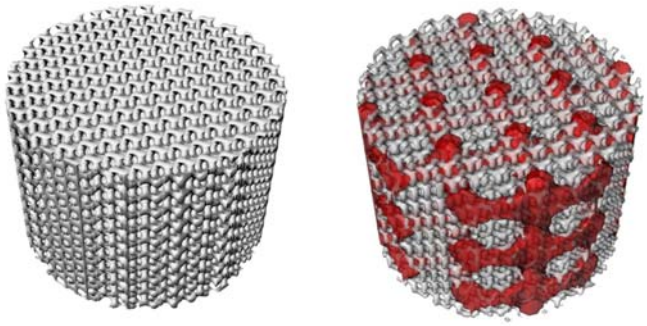

Fig. 10. **Original gyroid scaffold design (left) and novel gyroid scaffold design with integrated perfusion channels (right). The scaffold material and perfusion channels are co-visualised as semi-transparent layers.**

The scaffold design is based on the same gyroid pore architecture that was built and used in the seeding and culturing experiments, but now channels are included to avoid parts of the scaffold from being blocked by cells and deposited matrix at an early stage of cell culturing. The deducted channels are described by another minimal surface architecture, the primitive surface. Here, the channels form a cubic lattice and are described by the following boundary condition:

$$\cos(x/3) + \cos(y/3)+\cos(z/3)-\frac{1}{2}\left(\cos(x/3)\cos(y/3)-\cos(y/3)\cos(z/3)-\cos(z/3)\cos(x/3)\right)<0.94$$

The scaffold architecture presented here is designed to improve the transport of nutrients and oxygen. Furthermore, the network of larger-sized channels could facilitate the invasion of the host vasculature after implantation, or be employed for pre-vascularisation *in vitro*. The co-culture of myoblasts, endothelial cells and embryonic fibroblasts has been found to stimulate blood vessel formation in biodegradable polymer scaffolds *in vitro* [28]. The stereolithography technique enables to prepare designed scaffolds that direct pre-vascularisation and angiogenesis. Here, we suggest to make use of the designed larger channels for engineering a pre-fabricated vasculature. By first seeding and culturing iMSC in our designed scaffolds for several days, which is then followed by co-seeding of endothelial cells and embryonic fibroblasts in the still open meso-pore channels, endothelial vessel formation could be stimulated. Particularly for the engineering of tissues that require high levels of oxygen and nutrients, such as bone, the presented scaffold design and preparation technique are promising for future application.

Conclusions

It was shown that the open, accessible gyroid architecture of scaffolds fabricated by stereolithography improved cell seedability when compared to the tortuous pore architecture of scaffolds obtained by salt-leaching. The designed gyroid scaffolds can be wetted and intruded by a cell suspension more easily, resulting in a more homogeneous cell distribution. Dynamic seeding in

combination with high permeability results in the most homogeneous distribution of seeded cells. In static culturing, the open pore network architecture significantly delays the formation of a covering cell-sheet. As a result, scaffolds with high densities of relatively homogeneously distributed cells are obtained after dynamic seeding and 5 d of static culture. Here we show that by tuning the pore network architecture of a scaffold using rapid prototyping techniques such as stereolithography we can facilitate homogeneous cell distribution after seeding and prolong static culturing with sustained nutrient and oxygen accessibility. Novel scaffold designs with integrated perfusion channels are suggested to prevent large parts of the scaffolds from being blocked from medium in the generation of tissue grafts.

Acknowledgements

We would like to acknowledge the European Union (STEPS project, FP6-500465) and the TERM-Smart Mix program for funding.

References

1. Kim BS, Putnam AJ, Kulik TJ, Mooney DJ. Optimizing seeding and culture methods to engineer smooth muscle tissue on biodegradable polymer matrices. Biotechnology and Bioengineering. 1998;57(1):46-54.
2. Unsworth JM, Rose F, Wright E, Scotchford CA, Shakesheff KM. Seeding cells into needled felt scaffolds for tissue engineering applications. Journal of Biomedical Materials Research Part A. 2003;66A(2):425-431.
3. Li Y, Ma T, Kniss DA, Lasky LC, Yang ST. Effects of filtration seeding on cell density, spatial distribution, and proliferation in nonwoven fibrous matrices. Biotechnology Progress. 2001;17(5):935-944.
4. Xie J, Jung Y, Kim SH, Kim YH, Matsuda T. New technique of seeding chondrocytes into microporous poly(L-lactide-co-epsilon-caprolactone) sponge by cyclic compression force - Induced suction. Tissue Engineering. 2006;12(7):1811-1820.
5. VunjakNovakovic G, Freed LE, Biron RJ, Langer R. Effects of mixing on the composition and morphology of tissue-engineered cartilage. Aiche Journal. 1996;42(3):850-860.
6. Wendt D, Marsano A, Jakob M, Heberer M, Martin I. Oscillating perfusion of cell suspensions through three-dimensional scaffolds enhances cell seeding efficiency and uniformity. Biotechnology and Bioengineering. 2003;84(2):205-214.
7. Jukes JM, Moroni L, Van Blitterswijk CA, De Boer J. Critical steps toward a tissue-engineered cartilage implant using embryonic stem cells. Tissue Engineering Part A. 2008;14(1):135-147.

8. Dewez JL, Doren A, Schneider YJ, Rouxhet PG. Competitive adsorption of proteins: Key of the relationship between substratum surface properties and adhesion of epithelial cells. Biomaterials. 1999;20(6):547-559.
9. Malda J, Woodfield TBF, van der Vloodt F, Kooy FK, Martens DE, Tramper J, van Blitterswijk CA, et al. The effect of PEGT/PBT scaffold architecture on oxygen gradients in tissue engineered cartilaginous constructs. Biomaterials. 2004;25(26):5773-5780.
10. Freed LE, Vunjak-Novakovic G. Culture of organized cell communities. Advanced Drug Delivery Reviews. 1998;33(1-2):15-30.
11. IshaugRiley SL, Crane GM, Gurlek A, Miller MJ, Yasko AW, Yaszemski MJ, Mikos AG. Ectopic bone formation by marrow stromal osteoblast transplantation using poly(DL-lactic-co-glycolic acid) foams implanted into the rat mesentery. Journal of Biomedical Materials Research. 1997;36(1):1-8.
12. Martin I, Padera RF, Vunjak-Novakovic G, Freed LE. In vitro differentiation of chick embryo bone marrow stromal cells into cartilaginous and bone-like tissues. Journal of Orthopaedic Research. 1998;16(2):181-189.
13. Liu J, Barradas A, Fernandes H, Janssen F, Papenburg B, Stamatialis D, Martens AC, et al. In vitro and in vivo bioluminescence imaging of hypoxia in tissue engineered grafts. Tissue Engineering Part C-Methods. 2009;Epub ahead of print.
14. Wendt D, Stroebel S, Jakob M, John GT, Martin I. Uniform tissues engineered by seeding and culturing cells in 3D scaffolds under perfusion at defined oxygen tensions. Biorheology. 2006;43(3-4):481-488.
15. Volkmer E, Drosse I, Otto S, Stangelmayer A, Stengele M, Kallukalam BC, Mutschler W, et al. Hypoxia in static and dynamic 3D culture systems for tissue engineering of bone. Tissue Engineering Part A. 2008;14(8):1331-1340.
16. Sachlos E, Czernuszka JT. Making tissue engineering scaffolds work. Review on the application of solid freeform fabrication technology to the production of tissue engineering scaffolds. european Cells and Materials. 2003;5:29-40.
17. Clair JJ. Stereolithography and the biomedical engineering. Journal of Materials Processing Technology. 1996;57(3-4):393-396.
18. Melchels FPW, Feijen J, Grijpma DW. A poly(D,L-lactide) resin for the preparation of tissue engineering scaffolds by stereolithography. Biomaterials. 2009;30(23-24):3801-3809.
19. Mikos AG, Thorsen AJ, Czerwonka LA, Bao Y, Langer R, Winslow DN, Vacanti JP. Preparation and Characterization of Poly(L-Lactic Acid) Foams. Polymer. 1994;35(5):1068-1077.
20. Schoen AH. Infinite periodic minimal surfaces without self-intersections Springfield: Clearinghouse for Federal Scientific and Technical Information; 1970.
21. Schwarz HA. Gesammelte Mathematische Abhandlungen. Berlin: Springer-Verlag; 1890.
22. Yamazaki Y, Egawa K, Nose K, Kunimoto S, Takeuchi T. HIF-1-dependent VEGF reporter gene assay by a stable transformant of CHO cells. Biological & Pharmaceutical Bulletin. 2003;26(4):417-420.
23. Moroni L, Schotel R, Hamann D, de Wijn JR, van Blitterswijk CA. 3D fiber-deposited electrospun integrated scaffolds enhance cartilage tissue formation. Advanced Functional Materials. 2008;18(1):53-60.
[24]. Pêgo AP, Poot AA, Grijpma DW, Feijen J. Physical properties of high molecular weight 1,3-trimethylene carbonate and D,L-lactide copolymers. Journal of Materials Science: Materials in Medicine. 2003;14(9):767-773.
25. Mikos AG, Lyman MD, Freed LE, Langer R. Wetting of Poly(L-Lactic Acid) and Poly(Dl-Lactic-Co-Glycolic Acid) Foams for Tissue-Culture. Biomaterials. 1994;15(1):55-58.
26. Teixeira S, Fernandes H, Leusink A, van Blitterswijk C, Ferraz MP, Monteiro FJ, de Boer J. In vivo evaluation of highly macroporous ceramic scaffolds for bone tissue engineering. Journal of Biomedical Materials Research Part A. 2009;93(2):567-575.

27. Vander AJ, Sherman JH, Luciano DS. Human Physiology. New York: McGraw-Hill; 1985.
28. Levenberg S, Rouwkema J, Macdonald M, Garfein ES, Kohane DS, Darland DC, Marini R, et al. Engineering vascularized skeletal muscle tissue. Nature Biotechnology. 2005;23(7):879-884.